PHYSICAL REVIEW B, VOLUME 64, 161402(R)

Dynamical neutron-scattering measurements of residual stress in a Si crystal coated with a thin film

M. Agamalian,[1] E. Iolin,[1] H. Kaiser,[2] Ch. Rehm,[1] and S. A. Werner[2,3]
[1]*Oak Ridge National Laboratory, Oak Ridge, Tennessee 37831 and Argonne National Laboratory, Argonne, Illinois 60439**
[2]*University of Missouri-Columbia, Columbia, Missouri 65211*
[3]*National Institute of Standards and Technology, Gaithersburg, Maryland 20899*
(Received 19 July 2001; published 28 September 2001)

The residual stress in a thick Si(111) crystal coated with a 2000 Å thick Ni film was measured at the double-crystal diffractometer at Oak Ridge National Laboratory. The observed asymmetry of the back-face rocking curves and appearance of the garland reflections are related to the ultrasmall deformation strain induced by the Ni film. Relative deformation of the Si crystallographic cells in the vicinity of diffractive surfaces is $|\partial u_z/\partial z| \approx 1.6 \cdot 10^{-6}$. The radius of bending is ~19 km and the corresponding tension force applied to the Ni film is 90 ± 5 N/m.

DOI: 10.1103/PhysRevB.64.161402 PACS number(s): 62.20.−x, 61.12.Ex, 68.60.−p, 81.15.−z

In the past two decades, optical devices consisting of thin reflecting layers deposited on silicon or silicon-dioxide substrates, have found wide application in light, x-ray, and neutron diffraction. A significant surface-induced residual stress, which usually remains in the films as well as in the substrates after deposition, creates a serious limitation of quality of these devises. The residual stress in crystalline films can be detected directly by the conventional x-ray diffraction technique.[1] There exists another laser-based *in situ* technique, surface-stress-induced optical deflection (SSIOD), which is able to detect small deformation strain in substrates during the coating process.[2] The back-face neutron diffraction (BFND) from a perfect Si crystal, as it was shown in Refs. 3 and 4 is extremely sensitive to the ultrasmall deformation strain. This technique is capable of detecting residual stress in single crystals even when the relative deformation of the crystallographic cells is as small as $\sim 4 \cdot 10^{-7}$, which corresponds to the radius of bending of ~100 km. The radius of bending can be converted to the value of deformation of crystallographic cells in the film in a manner similar to the SSIOD technique,[2] however in contrary BFND works for final products. In the present work we describe the successful attempt to apply the BFND technique for detecting ultrasmall residual stress in a thick Si crystal coated with a thin Ni film.

The experiments were carried out using the double-crystal diffractometer at Oak Ridge National Laboratory[5] in the geometry similar to that described in Ref. 3 (see Fig. 1). The primary beam was diffracted from two premonochromators (are not shown in Fig. 1), and finally from a Si(111) triple-bounce channel-cut monochromator. The wavelength was $\lambda = 2.59$ Å and the beam cross-sectional area was 2 cm $\times$ 4 cm. The primary beam was restricted with a fixed vertical 1.8 mm wide Cd slit and the second scanning 4 mm wide slit was mounted directly in front of the detector. In this configuration, the intensity diffracted from different volumes within the crystal was mapped and the transmitted beam was used as a monitor signal for determination of the exact Bragg angle, θ_B, when the rocking curves were measured for positions other than the front face of the crystal.

A perfect Si(111) slab-shaped crystal with dimensions 114 mm $\times$ 40 mm $\times$ 8.1 mm was cut with the 114 mm $\times$ 40 mm diffractive surfaces parallel to the (111) crystallographic planes. The diffractive surfaces were polished mechanically, etched, and finally polished chemically; the surface metrology measurements were carried out using a laser figure interferometer. The root-mean-square height variation is 1.74 μm with the maximum peak-to-valley value of 7.88 μm. The front face (FF), back face (BF), and garland rocking curves (FFRC, BFRC, and GRC) shown in Fig. 1 were measured after the surface treatment. Then, one of the diffractive surfaces of the crystal was coated with a 2000 Å thick Ni film using a magnetron sputtering technique, and the neutron diffraction measurements were undertaken again. In both cases, the crystal under study was mounted on the rotation stage without external deformation strain.

According to the dynamical diffraction theory the Bragg reflection from a thick transparent perfect crystal occurs only from the front and back faces.[6] In the near vicinity of the exact Bragg angle the primary neutron beam reflects partly from the FF and partly penetrates inside the crystal propagating along straight trajectories and broadening (Bormann fan). The penetrated beam partly reflects from the BF (the first BF reflection) and partly leaves the crystal; this process repeats sequentially when the remaining inside the crystal neutron beam reaches the diffractive surfaces. Thus, one can conclude that the neutron wave propagates inside the crystal

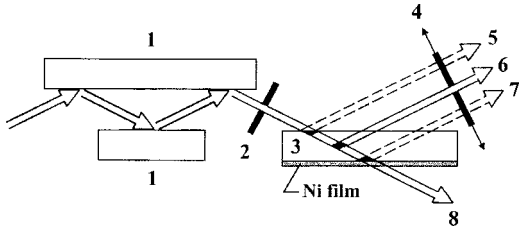

FIG. 1. Geometry of the experiment: 1 is the triple-bounce monochromator; 2, 4 are immovable and scanning Cd slits correspondingly; 3 is the Si(111) slab-shaped crystal coated with a 2000 Å Ni film; 5, 6, 7 are the FF, G, and BF reflections correspondingly; and 8 is the transmitted beam used as a monitor signal.

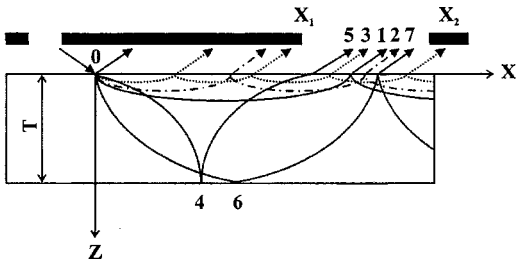

FIG. 2. The BF, 0-4-5, 0-6-7, and the garland, 0-1, 0-2, 0-3, trajectories in the deformed crystal; X_1, X_2 are the coordinates of the detector window aligned with respect to the BF reflected beam; and T is the crystal thickness.

in the direction parallel to the diffractive surfaces by sequential reflection from the front and back faces (BF-FF-BF- . . . mode). When the crystal is slightly deformed, the neutron trajectories inside the crystal are no longer straight. They become curved, which leads to the appearance of a second mode of propagation (in addition to the BF-FF-BF- . . . mode) created by so-called garland reflections only from the FF.[7] Our last theoretical analysis has shown that the garland mode gives significant contribution to the BF diffraction from a lightly-deformed crystal, thus it has been included in the last version of our model (see Fig. 2) originally developed in Ref. 3. The primary monochromatic beam collimated with a narrow cadmium slit partly reflects from the FF of a lightly-deformed crystal at $X=0$ and partly penetrates inside and splits on the BF-FF-BF- (see the trajectories 0-4-5 and 0-6-7), and on the garland mode (the trajectories 0-1, 0-2, and 0-3). Figure 2 demonstrates how the first BF reflection measured in our experiments becomes ''contaminated'' with the garland reflections (see the trajectories 5, 3, 1, 2, 7 passing through the detector slit X_1,X_2). However, the all curved trajectories in Fig. 2 are polygonal, when the crystal is not deformed, thus the garland mode does not exist in a perfect crystal and a ''pure'' first BF reflection can be detected.

The BF, $R_{\mathrm{BF}}(y)$, and garland, $R_{\mathrm{G}}(y)$, reflectivity functions were derived from the Takagi-Taupin equations,[8,9] which in the case of cylindrical deformation can be significantly simplified.[3] Here $y=(\theta-\theta_B)/\delta\theta_D$ is the dimensionless angular parameter of the dynamical diffraction theory and $\delta\theta_D$ is a half-width of the Darwin plateau.[6] Our model contains only one independent parameter of deformation, $b \sim \partial^2(\mathbf{HU})/\partial s_0 \partial s_h$, which is proportional to the gradient of the lattice constant. Here $\mathbf{H}$ is the vector of scattering, $H=4\pi \sin\theta_B/\lambda$,$\mathbf{U}$ is the displacement of nuclei under the deformation force, and $s_0=(X/\cos\theta_B+Z/\sin\theta_B)/2$, $s_h=(X/\cos\theta_B-Z/\sin\theta_B)/2$ are the coordinates directed along the incident and diffracted beams correspondingly. $R_G(y)$ was calculated numerically and $R_{\mathrm{BF}}(y)$, for $b>0$, $y<-1$, and $b>0$, $y>1+2bT$ (where $T=(T_1/\tau)\cdot\pi\cdot ctg\,\theta_B$ is the dimensionless crystal thickness, T_1 is the crystal thickness in μm, and $\tau\approx 77$ μm is the extinction length) obtained in analytical form using the geometrical optics approximation.

$$R_{\mathrm{BF}}(y)=\exp\{-2\arccos h[|y|-2bT\mathrm{sign}(y)]\}\times\{1-\exp[-2\arccos h(|y|)]\}^2\times H(X_r-X_1)H(X_2-X_r),$$

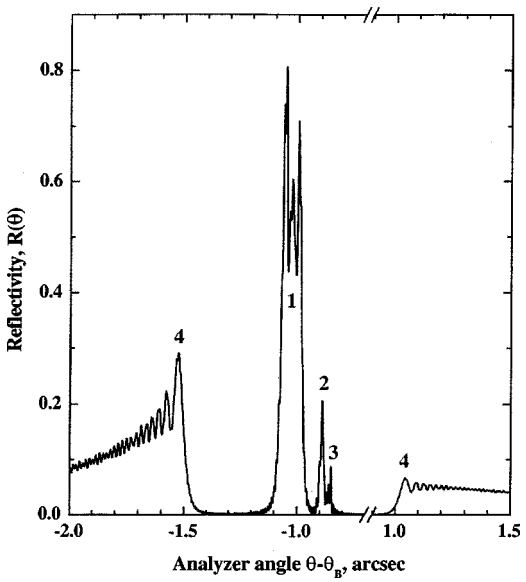

FIG. 3. The theoretical BF reflectivity curve calculated for the deformed crystal with $T=8.19$ mm and $b\approx 4\cdot 10^{-4}$. 1, 2, and 3 are the diffraction peaks related to the single-, double- and triple-bounce garland trajectories respectively; 4 are the wings of BF reflectivity function.

$$X_r=\frac{\mathrm{sign}(y)}{b}[\sqrt{y^2-1}-\sqrt{(|y|-2bT\mathrm{sign}(y))^2-1}]. \quad (1)$$

Here $H(X)$ is the Heaviside unit step function.

Figure 3 shows the theoretical total reflectivity functions, $R(y)=R_{\mathrm{BF}}(y)=R_{\mathrm{G}}(y)$, integrated over the detector slit X_1,X_2 (Fig. 2). This diagram demonstrates that the first BF reflection contains mostly the admixture of one-bounce garland reflection (peak 1), which gives significant contribution to the corresponding BFRC. It should be noted that the discrete spectrum of $R_G(y)$ (peaks 1, 2 and 3) appears only in the chosen geometry (see Fig. 2). The experimentally measurable BFRC or the GRC (see positions 6 and 7 in Fig. 1) is the convolution of the Darwin reflectivity function of the triple-bounce monochromator, $R_D^3(y)$, with the total reflectivity, $R(y)$:

$$I(\Delta)=\int R_D^3(y)\cdot R(y+\Delta)dy. \quad (2)$$

In the case of perfect crystal $R_{\mathrm{G}}(y)=0$ and $R(y)=R_{\mathrm{BF}}(y)$, thus only the ''pure'' symmetrical BFRC can be detected when the detector slit is in the position 7 (see Fig. 1). If the crystal is lightly deformed, $R(y)=R_{\mathrm{G}}(y)$ and $R(y)=R_{\mathrm{G}}(y)+R_{\mathrm{BF}}(y)$, thus a sharp peak appears for the position 6; the BFRC (position 7) becomes asymmetrical and ''contaminated'' with the garland mode.

The experimental BFRC obtained from the Si crystal without the Ni film is symmetric with respect to the exact Bragg angle, $\theta-\theta_B=0$, and the GRC contain only the detector background (see Fig. 4), that proves the quality of our Si substrate. The dramatic changes in the BFRCs and GRCs have been observed for the same crystal after depositing the 2000 Å Ni film on one of the diffractive surfaces (see Figs. 5

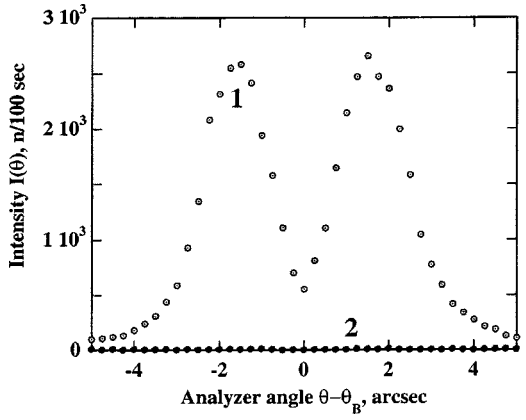

FIG. 4. The experimental BFRC (1) and GRC (2) measured from the perfect Si crystal before coating with the Ni film.

and 6). The BFRCs 1 and 2 (Fig. 5), measured for two orientations of the crystal (when the Ni-coated surface is set up as the BF (1) and then as the FF (2), are strongly asymmetrical, and in the cylindrical deformation approximation can be considered as mirror images of each other. The two diffractive surfaces of the crystal are not in principle optically identical due to the presence of the Ni film on one of them. However, the Bragg angle, $\theta_B = 24.4°$, is much larger than the critical angle of total reflection from Ni air interface ($\theta_c = 0.25°$ for $\lambda = 2.59$ Å), which completely excludes any possibility of total mirror reflection from the Ni film. Also, the absorption and any type of scattering from 2000 Å Ni film are vanishing small compared to the intensity of BF diffraction. The theoretical BFRCs, calculated from formulas (3) for the parameters $b \approx 4 \cdot 10^{-4}$ and $b \approx 3.5 \cdot 10^{-4}$, fit quite well to the corresponding experimental rocking curves. However, the experimental BFRCs do not contain the tiny peaks and steps resulting from the convolution of the main central peak of the BF reflectivity function (see Fig. 3) with that for the triple-bounce monochromator. This difference can easily be explained by the fact that the minimal angular step of the double-crystal diffractometer, $\Delta(\theta - \theta_B) = 0.25$ arcsec, is too large to resolve these tiny peculiarities of the BFRC profile. However, the main peak of garland reflections (see peak 1 in Fig. 3) contributes significantly to the intensity of the rocking curve and increases its asymmetry by $\sim 35\%$.

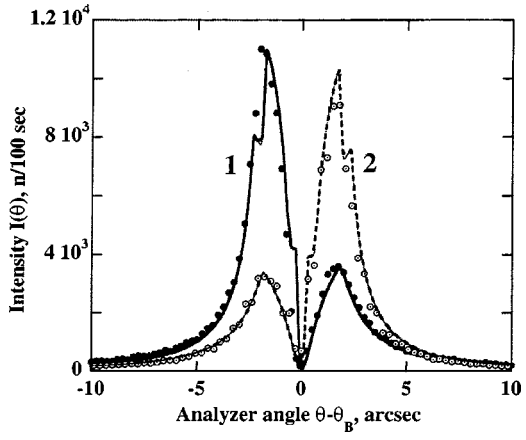

FIG. 5. The BFRCs measured after coating with the 2000 Å Ni film: 1, the Ni film is on the BF, as shown in Fig. 1; 2, the Ni coated surface is on the FF. Solid and dashed lines are the simulation curves calculated for $b = 4 \cdot 10^{-4}$ and $b = 3.5 \cdot 10^{-4}$, respectively.

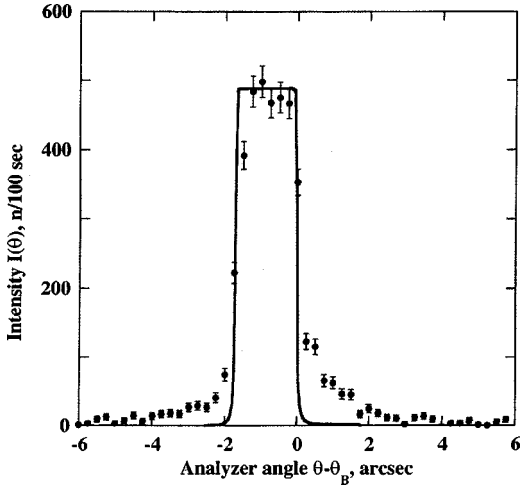

FIG. 6. The GRC measured from the crystal oriented as shown in Fig. 1 (Ni film is on the BF). Solid line is the simulation curve, calculated for $b \approx 3 \cdot 10^{-4}$.

Figure 6 shows the GRC measured when the Ni film was on the BF (see Fig. 1). The GRC peak, which practically coincides with the reflectivity function of the triple-bounce monochromator, is shifted from the exact Bragg position ($\theta - \theta_B = -1$ arcsec) in the direction of the bigger peak of the corresponding BFRC (see curve 1 in Fig. 5). Likewise, the GRC peak, being shifted in the opposite direction (not shown in Fig. 6), was detected for the second orientation of the crystal when the Ni film was on the FF. The theoretical GRC (solid line) fits rather well to the central part of the peak, but differs from that in the region of the wings. This deviation from the model of garland reflections, which are responsible for appearance of the GRC peak, is still the subject of discussion.

The parameter $b \approx 4 \cdot 10^{-4}$, determined from the best fits of the experimental BFRC, corresponds to the relative deformation of the Si crystallographic cells in the vicinity of diffractive surfaces, $|\partial u_z / \partial z| \approx 1.6 \cdot 10^{-6}$, and to the radius of bending, $R_b \approx (H/2b)(\tau/\pi)^2 \approx 19$ km, where τ is the extinction length.[3] The Stoney formula [1,2] converts the value of R_b to the tension force, f, applied to the film as a result of the substrate deformation:

$$f = ET^2/[6(1-\nu^2)R_b], \tag{3}$$

where $E \sim 10^{12}$ dyn/cm^2 is the modulus of elasticity, and ν is the Poisson constant of Si. Thus, the calculated value of f is 90 ± 5 N/m, which can be converted to units of the tensile strength, 427 MPa. This value is below the ultimate tensile strength of annealed bulk Ni, 586 MPa, but above the tensile yield strength of that, 345 MPa,[10] thus the 2000 Å Ni film under study is strongly strained (expanded along the X axis, Fig. 2). The value of f measured in our experiment is much

greater than the sensitivity limit of the BFND technique. The latter follows from the fact that the observed asymmetry of the BFRC (see Fig. 5) is very large and about two orders of magnitude weaker effect can be detected. The estimated sensitivity for our set-up was ~1 N/m; this value can be further optimized by changing the substrate thickness and the neutron wavelength.

The described experiments clearly show that the BFND can be used for residual stress measurements in thin films deposited on the diffractive surface. The BFND works similarly to the SSIOD *in situ* technique, detecting the deformation of the substrate, thus, it is capable to measure residual stress not only in crystalline, likewise the x-ray diffraction technique, but also in any amorphous, polymer, colloidal, mono- and multilayer thin films deposited on the diffractive surface of Si single crystals. The BFND is not an *in situ* technique and it allows evaluating the final product. We, therefore, expect its broad application, particularly in characterization of neutron and x-ray optical devices and even in the semiconductor industry using perfect Si crystals as test samples.

The authors thank L. Assoufid and R Khachatryan (Argonne National Laboratory) for surface metrology measurements. The submitted manuscript has been authored by a contractor of the U.S. Government under Contract No. DE-AC05-960R22464. Accordingly, the U.S. Government retains a nonexclusive, royalty-free license to publish or reproduce the published form of this contribution, or allow others to do so, for U.S. Government purposes. This research was in part supported by the Postdoctoral Research Associates Program administrated jointly by Oak Ridge National Laboratory and Oak Ridge Institute for Science and Education and the National Science Foundation. E. Iolin acknowledges support of a COBASE grant of the National Research Council of Missouri. S. A. Werner's work on the project is supported by NSF-PHY-9603559.

---

*Present address.

[1] I. C. Noyan, T. C. Huang, and B. R. York, Crit. Rev. Solid State Mater. Sci. **20(2)**, 125 (1995).

[2] M. Bicker, U. von Hülsen, U. Laudahn, A. Pundt, and U. Geyer, Rev. Sci. Instrum. **69**, 460 (1998).

[3] M. Agamalian, E. Iolin, L. Rusevich, C. J. Glinka, and G. D. Wignall, Phys. Rev. Lett. **81**, 602 (1998).

[4] M. Agamalian, E. Iolin, and G. D. Wignall, Neutron News **10**, 24 (1999).

[5] M. Agamalian, R. Triolo, and G. D. Wignall, J. Appl. Crystallogr. **30**, 345 (1997).

[6] W. H. Zachariasen, *Theory of X-ray Diffraction in Crystals* (Dover, New York, 1967).

[7] F. N. Chukhovskii and P. V. Petrashen, Acta Crystallogr. Sect. A **44**, 8 (1988).

[8] S. Takagi, Acta Crystallogr. **15**, 1311 (1962).

[9] D. Taupin, Bull. Soc. Fr. Mineral. Cristallogr. **84**, 51 (1961).

[10] G. S. Brady and H. R. Clauser, *Materials Handbook, Thirteenth Edition* (McGraw-Hill, New York, 1991).